

## Properties of a New Fluorescent Cytosine Analogue, Pyrrolocytosine

Katherine C. Thompson<sup>\*,†</sup> and Norimune Miyake<sup>‡</sup>

*School of Biological and Chemical Sciences, Birkbeck University of London, Malet Street, London WC1E 7HX, U.K., and Division of Physical and Inorganic Chemistry, University of Dundee, Dundee DD1 4HN, U.K.*

*Received: August 24, 2004; In Final Form: January 10, 2005*

Pyrrolocytosine is a novel, environment sensitive, fluorescent base that can be used in place of cytosine as a fluorescent marker in nucleic acids. In this work the results of a detailed computational investigation into the hybridization and photochemical properties of the base are reported. The interaction energy of the base pair formed between pyrrolocytosine and guanine, calculated at the MP2/6-31G(d,0.25)//HF/6-31G(d,p) level, was found to be  $-27.2$  kcal mol<sup>-1</sup>, comparing very favorably with the value calculated for the cytosine and guanine base pair,  $-25.8$  kcal mol<sup>-1</sup>. The wavelengths for the vertical transitions of pyrrolocytosine and cytosine were determined using both the configuration interaction technique, with singly excited configurations (CIS) and time-dependent density functional theory using the B3LYP functional (TDB3LYP). It was found that the spacing between the first  $\pi\pi^*$  state and the first  $n\pi^*$  state was significantly larger in the case of pyrrolocytosine than cytosine, providing a rationale for the higher fluorescence quantum yield of the former. Hydrogen bonding of pyrrolocytosine to guanine did not affect the predicted fluorescence properties of pyrrolocytosine whereas stacking guanine above pyrrolocytosine, in a manner appropriate to B-form DNA, significantly reduced the predicted fluorescence. Calculations on the two base systems using the TDB3LYP method produced low-lying charge-transfer states which are not predicted when the CIS method is used and are not thought to be physically meaningful.

### Introduction

Pyrrolocytosine is structurally similar to the natural nucleobase cytosine and can pair with guanine in a pseudo-Watson–Crick arrangement.<sup>1</sup> The spectroscopic properties of pyrrolocytosine are, however, markedly different from those of cytosine: the excitation maximum for pyrrolocytosine, which occurs at a wavelength of about 345 nm, is significantly red-shifted compared to that of cytosine at a wavelength of 267 nm and, unlike cytosine, pyrrolocytosine exhibits appreciable fluorescence, with a maximum at about 473 nm.<sup>1,2</sup> When pyrrolocytosine is incorporated into a nucleic acid, the fluorescence quantum yield observed is sensitive to the local structure of the biomolecule, potentially making pyrrolocytosine a very useful fluorescent probe in experimental studies of nucleic acid dynamics, and indeed this property has already been exploited by Liu and Martin<sup>3,4</sup> and by Lilley.<sup>5</sup> To better understand the fluorescence properties of pyrrolocytosine in nucleic acids, we present here the results of the first computational study of the properties of the base. Quantum chemical methods were used to examine both the extent to which pyrrolocytosine can mimic cytosine in a nucleic acid molecule and the spectral properties of pyrrolocytosine and cytosine. The electronic excited states of the bases were studied using the configuration interaction technique, with singly excited configurations (CIS) and time-dependent density functional theory, using the B3LYP<sup>6,7</sup> functional (TDB3LYP). The effects of both base stacking and hydrogen bonding on the fluorescence of pyrrolocytosine are reported. The results obtained at the CIS level are *qualitatively* different from those obtained using the TDB3LYP method, the

later only providing useful information only about low-lying locally excited states of the system.

### Calculation Methods

The Gaussian 98 and Gaussian 03 suites of programs were used for all calculations.<sup>8</sup> The software package Molekel<sup>9</sup> was used for visualization of the molecular geometries, vibrational frequencies and molecular orbitals. The calculations were performed either on a dual Xeon processor (2.6 GHz) machine with 4 GB of memory, running Linux or on a cluster of 6 HP ES40 computers, each with four 833 MHz EV68 processors and 8 GB of memory (Columbus cluster).

The ground-state geometry of pyrrolocytosine was optimized at both the HF/6-31G(d,p) and MP/6-31G(d,p) level with no symmetry restraints imposed. A frequency analysis was performed on the stationary points found to confirm that the optimized structures were true minima, characterized by real vibrational frequencies in all cases.

To determine the ability of pyrrolocytosine to mimic cytosine in a double-stranded helix, the energy of a pyrrolocytosine: guanine complex in a pseudo-Watson–Crick geometry was determined at the MP2/6-31G(d,0.25)//HF/6-31G(d,p) level. The input structure was generated by manually arranging the two bases, in their HF/6-31G(d,p) level optimized geometries, in a pseudo-Watson–Crick geometry. [The structure of guanine was optimized under  $C_s$  symmetry constraints.] The complex was optimized at the HF/6-31G(d,p) level, subject to  $C_s$  symmetry as planar structures would be expected in a helical environment. The energy of the optimized structure was determined at the MP2/6-31G(d,0.25) level with convergence criteria of the SCF equations set to  $1 \times 10^{-8}$  hartree. The 6-31G(d,0.25) basis set is a modified version of the standard Pople 6-31G(d) basis set

<sup>†</sup> Birkbeck University of London.

<sup>‡</sup> University of Dundee.

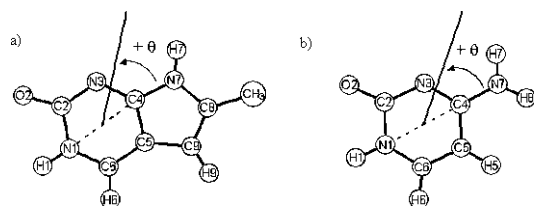


**Figure 1.** Structures of (a) pyrrolocytosine and (b) cytosine (with  $C_s$  symmetry) optimized at the MP2/6-31G(d,p) level. The N1–C4 axis, the midpoint of which is used as a reference for all angles for dipole moments, is shown. In the case of pyrrolocytosine the dipole moment is 7.61 D and  $\theta = -66^\circ$ , whereas for cytosine it is 7.40 D and  $\theta = -74^\circ$ .

where the exponent on the d function has been set to 0.25 rather than the value of 0.8 used in the standard basis set.<sup>10</sup> The interaction energy of the optimized structure, defined as the difference in energy between the complex and the individual bases in the same geometry as in the complex, was corrected for the basis set superposition error using the counterpoise correction method described in many standard texts.<sup>11</sup> This level of theory, MP2/6-31G(d,0.25)//HF/6-31G(d,p), with counterpoise-corrected interaction energies was selected because it has been used extensively to characterize other hydrogen-bonded structures, including the Watson–Crick cytosine:guanine complex.<sup>10,12,13</sup>

Vertical transition energies to low-lying singlet states were computed for pyrrolocytosine and cytosine using both the CIS and TDB3LYP methods. A range of basis functions were used to explore the influence of using a triple, rather than a double- $\zeta$  basis set, and the influence of using diffuse function. The basis sets employed were 6-31G(d,p), 6-31++G(d,p), 6-311++G(d,p), aug-cc-pVTZ, aug-cc-pVDZ, cc-pVTZ and cc-pVDZ. The fully optimized geometry of the first singlet  $\pi\pi^*$  state of pyrrolocytosine was determined at the CIS/6-31++G(d,p) level.

The fluorescence of pyrrolocytosine is significantly reduced in helical DNA compared to that of single-stranded DNA. To determine the physical origin of this change in fluorescence, the vertical transition energies and oscillator strengths were computed for complexes where (a) pyrrolocytosine was hydrogen bonded to guanine and (b) where pyrrolocytosine was stacked below guanine, as it would be in a section of B-form DNA. In the first instance the reference geometry used was the minimum energy structure of pyrrolocytosine hydrogen bonded to guanine located at the at the HF/6-31G(d,p) level, as described above. In the case of the stacked system a molecule of guanine, in a planar geometry optimized at the MP2/6-31G(d,p) level, was stacked above a molecule of pyrrolocytosine (also planar and optimized at the MP2/6-31G(d,p) level) so as to mimic the structure of B-form DNA, 3.375 Å rise per base and 36.00° twist per base. In both the hydrogen-bonded and the base-stacked cases two sets of vertical transition energies were computed: the first corresponding to pyrrolocytosine in its ground-state geometry, and hence providing data relevant to the absorption process, and the second corresponding to pyrrolocytosine in the optimized geometry of its first excited state, and hence providing data relevant to the fluorescence process.

## Results

**Ground-State Properties of Pyrrolocytosine.** Figure 1 shows the structure of pyrrolocytosine optimized at the MP2/6-31G(d,p) level, the structure of cytosine optimized with  $C_s$  symmetry imposed is shown for comparison. The magnitude and direction of the dipole moments are also given. Full geometric details of the optimized geometries of pyrrolocytosine

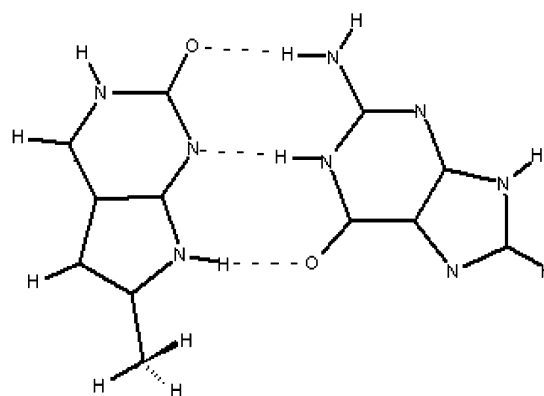


**Figure 2.** Structure of pyrrolocytosine hydrogen bonded to guanine in a pseudo-Watson–Crick fashion, optimized at the HF/6-31G(d,p) level.

**TABLE 1: Pertinent Details of the Geometry of the Hydrogen-Bonded Complex Formed between Pyrrolocytosine and Guanine Shown in Figure 2<sup>a</sup>**

H-bonded pair	interaction	distance (Å)/angle (deg)
pyrrolocytosine:guanine	O2...H)N2	3.12/179.3
	N3...H)N1	2.96/178.5
	N7(H)...O6	2.92/164.8
cytosine:guanine	O2...H)N2	3.02/178.1
	N3...H)N1	3.04/176.1
	N7(H)...O6	2.92/177.0

<sup>a</sup> The values reported by Šponer et al.,<sup>8</sup> for the corresponding complex formed between cytosine and guanine are given for comparison. All calculations were performed at the HF/6-31G(d,p) level.

determined at the HF/6-31G(d,p) and MP2/6-31G(d,p) levels are provided as Supporting Information. In both cases the ring systems are entirely planar, and the lowest energy conformer was found to possess  $C_s$  symmetry. Optimization of cytosine itself at the HF and MP2 level of theory leads to a slightly nonplanar structure, where the external  $-\text{NH}_2$  unit has a degree of pyramidalization;<sup>12</sup> however, pyrrolocytosine does not possess an external  $\text{NH}_2$  unit—the nitrogen forms part of a five-membered ring system.

Figure 2 shows the optimized structure of the pyrrolocytosine:guanine complex obtained at the HF/6-31G(d,p) level, under  $C_s$  symmetry. The Hessian matrix associated with the complex was found to contain no negative eigenvalues, indicating that a true minimum has been found and relaxing the  $C_s$  symmetry constraints did not lead to a lower energy complex being located. Table 1 provides pertinent details regarding the geometry of the hydrogen-bonded complex. The full structure of the pyrrolocytosine:guanine complex is provided as Supporting Information. The counterpoise corrected interaction energy of the complex at the MP2/6-31G(d,0.25)//HF/6-31G(d,p) levels was found to be  $-27.2 \text{ kcal mol}^{-1}$ , similar to the value reported for the Watson–Crick cytosine:guanine complex calculated at this level:  $-25.8 \text{ kcal mol}^{-1}$ .<sup>10</sup> As expected, the magnitude of the counterpoise correction was found to be much larger at the MP2 level than at the HF level;<sup>12</sup> however, at both the MP2 and the HF level the difference in the interaction action energies of the pyrrolocytosine:guanine complex and the cytosine:guanine complex is similar whether counterpoise corrected or uncorrected interaction energies are compared. No experimental results have yet been reported in the literature on the structure of the pyrrolocytosine:guanine complex but Berry et al.<sup>1</sup> report that replacing up to four cytosine units with pyrrolocytosine in duplexes of fully complementary deoxyribonucleotides does not change the melting temperature of the duplexes, indicating that the use of the fluorescent marker pyrrolocytosine in place of

**TABLE 2: Vertical Transition Energies,  $E$ , Oscillator Strengths,  $f$ , and Polarization Angles for the  $\pi\pi^*$  Transitions,  $\theta$  (As Defined in Figure 1), Predicted at the CIS Level of Theory<sup>a</sup>**

	pyrrolocytosine				cytosine			
	$E/\text{eV}$	$f$	$\theta/\text{deg}$	assignment	$E/\text{eV}$	$f$	$\theta/\text{deg}$	assignment
CIS/6-311++G(d,p)								
1st transition	3.43	0.274	−115	$\pi\pi^*$	4.33	0.173	+34	$\pi\pi^*$
2nd transition	3.77	0.000		Rydberg	4.59	0.012		Rydberg
3rd transition	4.11	0.001		Rydberg	4.92	0.003		$n\pi^*$
4th transition	4.32	0.003		Rydberg	5.06	0.000		Rydberg
5th transition	4.44	0.054	−8	$\pi\pi^*$	5.20	0.000		$n\pi^*$
6th transition	4.66	0.002		Rydberg	5.22	0.018		Rydberg
7th transition	4.71	0.001		Rydberg	5.29	0.315	+148	$\pi\pi^*$
8th transition	4.71	0.060	−29	$\pi\pi^*$	5.35	0.000		Rydberg
9th transition	4.77	0.004		$n\pi^*$	5.54	0.645	+121	$\pi\pi^*$
CIS/6-31++G(d,p)								
1st transition	3.46	0.279	−115	$\pi\pi^*$	4.36	0.173	+33	$\pi\pi^*$
2nd transition	3.77	0.001		Rydberg	4.57	0.014		Rydberg
3rd transition	4.10	0.002		Rydberg	4.94	0.002		$n\pi^*$
4th transition	4.31	0.004		Rydberg	5.05	0.000		Rydberg
5th transition	4.45	0.052	−7	$\pi\pi^*$	5.20	0.017		Rydberg
6th transition	4.67	0.001		Rydberg	5.21	0.002		$n\pi^*$
7th transition	4.69	0.002		Rydberg	5.31	0.314	+148	$\pi\pi^*$
8th transition	4.73	0.056	−28	$\pi\pi^*$	5.35	0.000		Rydberg
9th transition	4.79	0.004		$n\pi^*$	5.56	0.650	+120	$\pi\pi^*$
CIS/6-31G(d,p)								
1st transition	3.54	0.299	−117	$\pi\pi^*$	4.46	0.164	+32	$\pi\pi^*$
2nd transition	4.79	0.044	−21	$\pi\pi^*$	4.96	0.002		$n\pi^*$
3rd transition	4.80	0.003		$n\pi^*$	5.21	0.001		$n\pi^*$
CIS/aug-cc-pVTZ								
1st transition	3.40	0.254	−115	$\pi\pi^*$	4.30	0.169	+33	$\pi\pi^*$
2nd transition	3.70	0.000		Rydberg	4.54	0.013		Rydberg
3rd transition	4.04	0.001		Rydberg	4.94	0.002		$n\pi^*$
4th transition	4.22	0.003		Rydberg	5.01	0.001		Rydberg
5th transition	4.24	0.034		Rydberg <sup>b</sup>	5.19	0.015		Rydberg
6th transition	4.52	0.002		Rydberg	5.24	0.000		$n\pi^*$
7th transition	4.58	0.001		Rydberg	5.25	0.002		Rydberg
8th transition	4.64	0.074	−24	$\pi\pi^*$	5.26	0.269	+150	$\pi\pi^*$
9th transition	4.78	0.004		$n\pi^*$	5.37	0.236	+114	$\pi\pi^*$
CIS/aug-cc-pVDZ								
1st transition	3.40	0.256	−115	$\pi\pi^*$	4.30	0.169	+32	$\pi\pi^*$
2nd transition	3.71	0.000		Rydberg	4.53	0.013		Rydberg
3rd transition	4.05	0.001		Rydberg	4.95	0.002		$n\pi^*$
4th transition	4.24	0.004		Rydberg	5.00	0.001		Rydberg
5th transition	4.32	0.041		Rydberg <sup>b</sup>	5.18	0.018		Rydberg
6th transition	4.58	0.002		Rydberg	5.23	0.001		$n\pi^*$
7th transition	4.61	0.001		Rydberg	5.26	0.279	+149	$\pi\pi^*$
8th transition	4.66	0.060	−26	$\pi\pi^*$	5.27	0.001		Rydberg
9th transition	4.79	0.004		$n\pi^*$	5.46	0.502	−40	$\pi\pi^*$
CIS/cc-pVTZ								
1st transition	3.46	0.286	−119	$\pi\pi^*$	4.37	0.171	+30	$\pi\pi^*$
2nd transition	4.70	0.056	−21	$\pi\pi^*$	4.97	0.002		$n\pi^*$
3rd transition	4.79	0.002		$n\pi^*$	5.25	0.000		$n\pi^*$
CIS/cc-pVDZ								
1st transition	3.51	0.301	−119	$\pi\pi^*$	4.43	0.166	+30	$\pi\pi^*$
2nd transition	4.77	0.046	−21	$\pi\pi^*$	4.97	0.002		$n\pi^*$
3rd transition	4.79	0.002		$n\pi^*$	5.21	0.000		$n\pi^*$

<sup>a</sup> All energies have been scaled by a factor of 0.72. States with significant Rydberg or  $\sigma^*$  character are simply assigned “Rydberg”. The MP2/6-31G(d,p)  $C_s$  optimized geometries were used for all calculations. <sup>b</sup> This transition has some  $\pi\pi^*$  character but is highly contaminated with Rydberg character.

cytosine in a nucleic acid does not measurably change the stability of the nucleic acid.

**Vertical Transition Energies: Single Base Studies.** Table 2 gives the vertical transition energies, oscillator strengths, and where appropriate, transition polarization angles for pyrrolocytosine and cytosine calculated for the  $C_s$ , MP2/6-31G(d,p) optimized geometries using the CIS method and each of the basis sets investigated. Transitions up to the first  $n\pi^*$  state of pyrrolocytosine have been included. The transition energies have been scaled using a constant factor of 0.72, as suggested by Broo and Holmén.<sup>14</sup> Table 3 gives the corresponding information for calculations performed at the TDB3LYP level. As can be seen from Tables 2 and 3, the predicted vertical transition

energies and dipoles hardly change upon going from the 6-31++G(d,p) basis set to the 6-311++G(d,p) basis set, nor from the aug-cc-pVDZ to the aug-cc-pVTZ. The predicted ordering of the states does not change at all in the case of pyrrolocytosine and for cytosine itself the only change is a switch in the order of two very closely spaced states. It thus seems sensible to conclude that the extra computational effort required to use a triple- $\zeta$ , rather than a double- $\zeta$ , basis set is not justified. The use of diffuse functions does, however, appear to be justified. Two observations can be made by comparing the results at the 6-31++G(d,p) and 6-31G(d,p) levels, the aug-cc-pVTZ and cc-pVTZ levels and the aug-cc-pVDZ and cc-pVDZ levels: First, the inclusion of diffuse functions leads to

**TABLE 3: Vertical Transition Energies,  $E$ , Oscillator Strengths,  $f$ , and Polarization Angles for the  $\pi\pi^*$  Transitions,  $\theta$  (As Defined in Figure 1), Predicted at the TDB3LYP Level of Theory<sup>a</sup>**

	pyrrolocytosine				cytosine			
	$E/\text{eV}$	$f$	$\theta/\text{deg}$	assignment	$E/\text{eV}$	$f$	$\theta/\text{deg}$	assignment
TDB3LYP/6-311++G(d,p)								
1st transition	3.50	0.071	+23	$\pi\pi^*$	4.61	0.037	+45	$\pi\pi^*$
2nd transition	4.34	0.000		$n\pi^*$	4.73	0.001		$n\pi^*$
3rd transition	4.50	0.000		Rydberg	5.10	0.001		$n\pi^*$
4th transition	4.65	0.000		Rydberg	5.23	0.005		Rydberg
5th transition	4.83	0.001		$n\pi^*$	5.37	0.083	+154	$\pi\pi^*$
6th transition	4.97	0.002	-26	$\pi\pi^*$	5.61	0.000		$n\pi^*$
7th transition	5.18	0.003		Rydberg	5.63	0.001		Rydberg
8th transition	5.21	0.100	-38	$\pi\pi^*$	5.77	0.003		Rydberg
9th transition	5.47	0.000		Rydberg	5.86	0.014		Rydberg
TDB3LYP/6-31++G(d,p)								
1st transition	3.53	0.073	+24	$\pi\pi^*$	4.64	0.038	+45	$\pi\pi^*$
2nd transition	4.37	0.000		$n\pi^*$	4.77	0.001		$n\pi^*$
3rd transition	4.45	0.000		Rydberg	5.14	0.000		$n\pi^*$
4th transition	4.61	0.000		Rydberg	5.18	0.006		Rydberg
5th transition	4.86	0.001		$n\pi^*$	5.40	0.080	+154	$\pi\pi^*$
6th transition	5.00	0.001	-25	$\pi\pi^*$	5.57	0.001		Rydberg
7th transition	5.13	0.003		Rydberg	5.65	0.000		$n\pi^*$
8th transition	5.21	0.091	-39	$\pi\pi^*$	5.70	0.003		Rydberg
9th transition	5.43	0.000		Rydberg	5.82	0.015		Rydberg
TDB3LYP/6-31G(d,p)								
1st transition	3.58	0.073	+24	$\pi\pi^*$	4.69	0.030	+44	$\pi\pi^*$
2nd transition	4.29	0.000		$n\pi^*$	4.74	0.000		$n\pi^*$
3rd transition	4.82	0.001		$n\pi^*$	5.13	0.002		$n\pi^*$
TDB3LYP/aug-cc-pVTZ								
1st transition	3.48	0.068	-2	$\pi\pi^*$	4.60	0.038	+44	$\pi\pi^*$
2nd transition	4.32	0.000		$n\pi^*$	4.73	0.001		$n\pi^*$
3rd transition	4.44	0.000		Rydberg	5.11	0.000		$n\pi^*$
4th transition	4.61	0.000		Rydberg	5.19	0.005		Rydberg
5th transition	4.82	0.001		$n\pi^*$	5.36	0.079	+154	$\pi\pi^*$
6th transition	4.95	0.003	-27	$\pi\pi^*$	5.56	0.000		Rydberg
7th transition	5.08	0.002		Rydberg	5.61	0.000		$n\pi^*$
8th transition	5.13	0.068	-39	$\pi\pi^*$	5.73	0.004		Rydberg
9th transition	5.35	0.000		Rydberg	5.81	0.014		Rydberg
TDB3LYP/aug-cc-pVDZ								
1st transition	3.48	0.068	-2	$\pi\pi^*$	4.60	0.038	+44	$\pi\pi^*$
2nd transition	4.31	0.000		$n\pi^*$	4.73	0.001		$n\pi^*$
3rd transition	4.43	0.000		Rydberg	5.12	0.000		$n\pi^*$
4th transition	4.60	0.000		Rydberg	5.17	0.005		Rydberg
5th transition	4.83	0.001		$n\pi^*$	5.36	0.077	+153	$\pi\pi^*$
6th transition	4.95	0.002	-27	$\pi\pi^*$	5.55	0.001		Rydberg
7th transition	5.09	0.003		Rydberg	5.60	0.000		$n\pi^*$
8th transition	5.14	0.078	-39	$\pi\pi^*$	5.71	0.004		Rydberg
9th transition	5.37	0.000		Rydberg	5.80	0.014		Rydberg
TDB3LYP/cc-pVTZ								
1st transition	3.52	0.073	-2	$\pi\pi^*$	4.66	0.034	+41	$\pi\pi^*$
2nd transition	4.31	0.000		$n\pi^*$	4.75	0.000		$n\pi^*$
3rd transition	4.83	0.001		$n\pi^*$	5.14	0.001		$n\pi^*$
TDB3LYP/cc-pVDZ								
1st transition	3.55	0.075	-2	$\pi\pi^*$	4.68	0.030	+42	$\pi\pi^*$
2nd transition	4.25	0.000		$n\pi^*$	4.71	0.000		$n\pi^*$
3rd transition	4.80	0.001		$n\pi^*$	5.12	0.001		$n\pi^*$

<sup>a</sup> The MP2/6-31G(d,p)  $C_s$  optimized geometries were used for all calculations. States with significant Rydberg or  $\sigma^*$  character are simply assigned "Rydberg".

the prediction of Rydberg like states not otherwise predicted. This result is not unexpected, as it is well-known that the inclusion of diffuse functions is essential when looking at Rydberg states.<sup>15</sup> Perhaps more interesting though is the effect that adding diffuse functions has on the relative energies of the  $\pi\pi^*$  and  $n\pi^*$  states. Table 2 clearly shows that when the CIS method is used the inclusion of diffuse functions lowers the energy of the  $\pi\pi^*$  states for both pyrrolocytosine and cytosine, but scarcely changes the energy of  $n\pi^*$  states. Table 3 shows the results obtained in this work using the TDB3LYP method: not only does the use of diffuse functions lower the predicted energy of the  $\pi\pi^*$  states, but it also tends to slightly increase the predicted energy of the  $n\pi^*$  states. A similar result has been

found previously for cytosine when the TDB3LYP method is used.<sup>16</sup> Thus the inclusion of diffuse functions is necessary not only for the treatment of Rydberg states but also to accurately predict the spacing between valence states, and hence the possible decay pathways open to a base.

The suitability of the TDB3LYP method for studying this system will now be considered. The first transition of pyrrolocytosine is predicted to be to a  $\pi\pi^*$  state by both the CIS and the TDB3LYP methods. After scaling, the CIS level calculations give a value similar to that from the TDB3LYP level calculations for the vertical transition energy to the  $\pi\pi^*$  state: 3.46 and 3.53 eV, respectively, when the 6-31++G(d,p) basis set is used. No gas-phase experimental data are available to compare



with these predicted values, but the excitation spectra of aqueous solutions of oligonucleotides containing one pyrrolocytosine unit have two strong peaks, one at 345 nm, 3.59 eV, and one at 272 nm, 4.56 eV.<sup>5</sup> Thus both methods, CIS and TDB3LYP, accurately predict the position of the first band. However, whereas the CIS method predicts a second strong absorption at 4.45 eV, the second peak predicted to have any significant intensity by the TDB3LYP method is at 5.52 eV, around 1 eV too high. It appears that the CIS method gives results more consistent with the limited experimental values.

**Different Spectral Properties of Pyrrolocytosine and Cytosine.** The spectral properties of pyrrolocytosine are clearly very different from those of cytosine, despite the structural similarities of the two compounds. It has long been known that although cytosine absorbs strongly in the UV, it exhibits only very weak fluorescence.<sup>17</sup> Explanations, based on quantum mechanical studies, for the radiationless decay of cytosine have recently been provided by Shukla and Leszczynski<sup>16</sup> and by Ismail et al.<sup>18</sup> In both cases the underlying reason proposed for the exceptionally low fluorescence quantum yield of cytosine is that although a  $\pi\pi^*$  state is the lowest energy state accessible via a vertical transition from the ground state, the relaxed (optimized) geometry of this  $\pi\pi^*$  state is in fact higher in energy than the relaxed geometry of the first  $n\pi^*$  state, making a state crossing from the initially formed  $\pi\pi^*$  state to the  $n\pi^*$  state likely. Ismail et al. located a conical intersection linking the  $n\pi^*$  state to the ground state, thus providing an accessible radiationless deactivation route for cytosine and an explanation for the low fluorescence quantum yield of cytosine. In the case of pyrrolocytosine, the vertical transition energy to the first  $n\pi^*$  state lies 1.33 eV higher in energy than that to the lowest  $\pi\pi^*$  state, compared to 0.58 eV in the case of cytosine (see Table 2). Although the fully optimized geometry of the lowest energy  $n\pi^*$  state of pyrrolocytosine was not located in this work, the geometry optimized under  $C_s$  symmetry constraints was located and found to be 1.02 eV higher in energy than that of the optimized lowest energy  $\pi\pi^*$  state, when optimized under  $C_s$  symmetry constraints. Considering that the energy of the  $\pi\pi^*$  state only dropped by 0.01 eV when the symmetry requirements were relaxed, it is very unlikely therefore that the fully relaxed  $n\pi^*$  state would lie lower in energy than the relaxed  $\pi\pi^*$  state, and thus a state switch from an initially formed  $\pi\pi^*$  state to an  $n\pi^*$ , as proposed by Shukla and Leszczynski, and Ismail for cytosine, is not expected in the case of pyrrolocytosine. A more recent paper by Merchán and Serrano-Andrés,<sup>19</sup> studied the nonradiative deactivation of cytosine at a higher level of theory than Ismail et al. and concluded that radiationless decay of cytosine occurred via a conical intersection linking the  $\pi\pi^*$  state to the ground state. As pyrrolocytosine shows appreciably more fluorescence than cytosine it can be concluded that if a similar conical intersection links the  $\pi\pi^*$  state of pyrrolocytosine to the ground state, then the barrier between the relaxed  $\pi\pi^*$  state structure and the conical intersection must be considerably larger than the 2.5 kcal mol<sup>-1</sup> calculated by Merchán and Serrano-Andrés in the case of cytosine.

**Optimized Excited-State Structure.** The structure of the lowest energy singlet  $\pi\pi^*$  state of pyrrolocytosine,  $S_1$ , was optimized at the CIS/6-31++G(d,p) level. The orbitals involved in the transition from the ground state to  $S_1$  are shown in Figure 3. The fully optimized structure, characterized by all positive frequencies, is not completely planar. Table 4 gives the geometric parameters of the ground state and the first excited state. The calculated dipole moment of the fully optimized  $\pi\pi^*$  state is 8.07 D, the dipole moment of the fully optimized ground

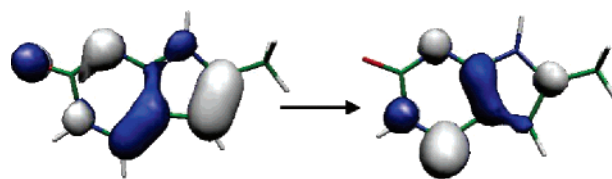


Figure 3. Orbitals involved in first  $\pi\pi^*$  transition of pyrrolocytosine.

TABLE 4: Geometry of the Ground State and Optimized Lowest Energy Excited State, a  $\pi\pi^*$  State, of Pyrrolocytosine (Bond Lengths in Å; Bond Angles in Degrees)

	ground state	$\pi\pi^*$ state	difference
C2N1	1.43	1.42	-0.01
N3C2	1.38	1.37	-0.01
C4N3	1.32	1.31	-0.01
C5C4	1.44	1.42	-0.02
C6C5	1.37	1.41	+0.04
N1C6	1.35	1.36	+0.01
C2O	1.23	1.20	-0.03
N7C4	1.37	1.38	+0.01
C8N7	1.40	1.34	-0.06
C9C8	1.37	1.41	+0.04
C5C9	1.44	1.40	-0.04
C10C8	1.49	1.49	0.00
N1C2N3	116.0	119.1	+3.1
C2N3C4	116.3	115.0	-1.3
N3C4C5	129.1	128.6	-0.5
C4C5C6	114.6	116.3	+1.7
C2N1C6	126.7	124.5	-2.2
OC2N3	126.2	124.3	-1.9
N3C4N7	124.9	124.0	-0.9
C4N7C8	110.4	110.5	+0.1
N7C8C9	109.1	108.1	-1.0
C4C5C9	107.7	106.8	-0.9
N7C8C10	120.5	122.6	+2.1
N1C6C5C4	0.0	9.8	+9.8
N3C2N1C6	0.0	12.8	+12.8
C4N3C2N1	0.0	0.3	+0.3
C5C4N3C2	0.0	-7.7	-7.7
C6C5C4N3	0.0	2.5	+2.5
OC2N1C6	180.0	-168.0	-12.0
N7C4N3C2	180.0	-178.7	-1.3
N7C8C9C5	0.0	-0.6	-0.6
C10C8C9C5	180.0	-176.0	-4.0

state at the same level, MP2/6-31++G(d,p), is 7.90 D; i.e., the excited state is slightly more polar than the ground state. The difference in energy between the optimized ground state and the optimized first excited state is 3.23 eV, compared to the vertical transition energy from the ground state of 3.46 eV. The vertical transition energy from the optimized excited state to the ground state is 2.98 eV and has an associated oscillator strength of 0.256. Thus fluorescence from pyrrolocytosine would be expected to occur around 2.98 eV, 416 nm. There are no gas-phase studies to compare this value with. Fluorescence from an aqueous solution of oligonucleotides containing pyrrolocytosine has been reported to peak at about 473 nm,<sup>1</sup> which is close to the value predicted here for the fluorescence of pyrrolocytosine in vacuo.

**Vertical Transition Energies: Hydrogen-Bonded Complexes.** The vertical transition energies and associated oscillator strengths were computed for the hydrogen-bonded complex of pyrrolocytosine and guanine. Table 5 gives the results for the low-lying valence states and charge-transfer states (for which the transition corresponds to an electron being promoted from an orbital centered on pyrrolocytosine to a vacant orbital centered on guanine or vice versa). Details of the corresponding transitions of the bases alone in the complex geometry have also been provided where appropriate. Table 5 illustrates several interesting features. The first concerns the effect of hydrogen

**TABLE 5: Vertical Transitions Energies,  $E$ , and Oscillator Strengths,  $f$ , to Low-Lying States of the Hydrogen-Bonded Complex of Pyrrolocytosine and Guanine Computed Optimized at the HF/6-31G(d,p) Level<sup>a</sup>**

	pyrrolocytosine (PC) hydrogen bonded to guanine (G)			monomer alone in complex geometry	
	$E/\text{eV}$	$f$	assignment	$E/\text{eV}$	$f$
CIS/6-31++G(d,p)					
1st transition	3.65	0.284	$\pi\pi^*$ on PC	3.66	0.274
2nd transition	4.52	0.159	$\pi\pi^*$ on G	4.49	0.291
TDB3LYP/6-31++G(d,p)					
1st transition	3.25	0.000	CT ( $\pi_{\text{G}}\pi_{\text{PC}}^*$ )		
2nd transition	3.70	0.072	$\pi\pi^*$ on PC	3.71	0.071

<sup>a</sup> The transition energies for the individual bases in the complex geometry are also given. The transition energies calculated at the CIS level have been scaled by a factor of 0.72. Transitions with charge-transfer character are reported as CT.

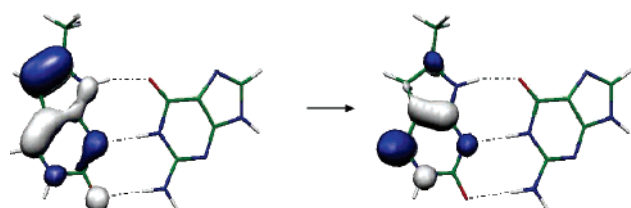


**Figure 4.** Pyrrolocytosine hydrogen bonded to guanine. At the CIS level orbitals involved in first  $\pi\pi^*$  transition are located on the pyrrolocytosine unit only.

bonding on the energy of the first localized  $\pi\pi^*$  state of pyrrolocytosine. Initially, hydrogen bonding appears to increase the energy of this  $\pi\pi^*$  state, from 3.46 to 3.65 eV at the CIS level and from 3.53 to 3.70 eV at the TDB3LYP level. However, closer inspection of Table 5 reveals that the increase in energy of the  $\pi\pi^*$  state is in fact caused by the distortion in the geometry of pyrrolocytosine that occurs when it bonds to guanine in the optimal geometry of the complex as a whole. Hydrogen bonding itself appears to significantly affect neither the energy nor the oscillator strength of the vertical transition to the  $\pi\pi^*$  state change.

The second feature of interest in Table 5 is the ordering of the states. Whereas the first excited state of the hydrogen-bonded complex computed at the CIS level is essentially identical to the first transition of pyrrolocytosine alone, the orbitals involved are shown in Figure 4, the first transition predicted at the TDB3LYP level is of charge-transfer nature, involving the promotion of an electron from the HOMO of guanine to the LUMO of pyrrolocytosine. At the CIS level, transition energies for states lying up to 4.72 eV (scaled) above the ground state were calculated and no charge-transfer states were identified. It can therefore be concluded that the state predicted by the TDB3LYP method to occur at 3.13 eV is predicted by the CIS method to lie above 4.72 eV, indicating that the two methods are in disagreement by over 1.5 eV as to the energy of the first charge-transfer state. A number of groups have previously reported that states of charge-transfer character are not correctly described using time-dependent density functional theory with local exchange-correlation functionals (such as the B3LYP functional), as the functional potentials do not fall off with  $1/r$  (where  $r$  is the nucleus–electron distance), as they should at large distances from the nucleus.<sup>20–25</sup> Thus, although the TDB3LYP method has previously been used to study the fluorescent base 2-aminopurine in base stacked structures,<sup>26,27</sup> the method should be used with caution as it tends to predict states of charge-transfer character that are unrealistically low in energy and are best disregarded.

Both the CIS and TDB3LYP methods are in agreement that neither the energy nor the oscillator strength of the vertical transition to the lowest energy  $\pi\pi^*$  state is affected by hydrogen bonding. To determine the influence of hydrogen bonding on

the fluorescence of pyrrolocytosine, however, the vertical transition that should be considered is the one from the relaxed (optimized) geometry of the  $\pi\pi^*$  state to the ground state. A complete optimization of the  $\pi\pi^*$  state of the hydrogen-bonded complex is not computationally feasible at the present time. However, as has been stated above, the transition is essentially a localized one, concerning orbitals centered on the pyrrolocytosine unit only. Thus details of the fluorescence from the hydrogen-bonded structure can be obtained by studying the optimized first excited state of pyrrolocytosine,  $S_1$ , in a hydrogen-bonded arrangement with guanine in its ground-state geometry. The results presented in Table 6 demonstrate that hydrogen bonding of pyrrolocytosine in its  $S_1$  geometry to guanine has very little effect on either the energy of the  $\pi\pi^*$  state or the oscillator strength for the transition. Thus it can be concluded that neither the absorption nor the fluorescence intensity of pyrrolocytosine should be affected by hydrogen bonding. It should be mentioned at this point that the structure of the complex used for these calculations was a ground-state structure optimized at the HF/6-31G(d,p) level. Optimization of the pyrrolocytosine:guanine complex at the MP2/6-31G(d,p) level, that is, including the effects of electron correlation in the optimization, produces a structure in which the hydrogen bonds are  $\sim 0.1$  Å shorter than those obtained at the HF/6-31G(d,p) level. The smaller separation of the two bases predicted at the MP2 level could favor intermolecular charge transfer.

#### Vertical Transition Energies: Based Stacked Complexes.

The energies and oscillator strengths calculated for the low-lying valence and charge-transfer states of the complex where a molecule of guanine is stacked above pyrrolocytosine as it would be in B-form DNA are reported in Table 7. The complex used is shown in Figure 5 and the full structure is provided within the Supporting Information. As can be seen from Table 7, in this case although the TDB3LYP does predict a low-lying charge-transfer state at 3.75 eV, the lowest lying state computed using both the CIS and TDB3LYP methods is the  $\pi\pi^*$  state corresponding to a electron being promoted between essentially the same orbitals as those shown in Figure 3. Both methods show that although the energy of this state is unaffected by the presence of the guanine molecule stacked above the pyrrolocytosine, the oscillator strength for the transition reduced by about 25%. The predicted fluorescence of pyrrolocytosine when in the base-stacked complex was studied by replacing the ground state optimized structure of pyrrolocytosine shown in Figure 4, with the optimized structure of pyrrolocytosine in its first excited state,  $S_1$ . The results of these calculations, shown in Table 6, demonstrate that whereas hydrogen bonding of pyrrolocytosine to guanine does not change the predicted oscillator strength for the fluorescence of pyrrolocytosine, stacking a molecule of guanine above pyrrolocytosine as it would be in B-form DNA reduces the predicted oscillator strength of the fluorescence transition by nearly 20%. As the oscillator strength for a

**TABLE 6: Energies,  $E$ , and Oscillator Strengths,  $f$ , Calculated for the First Vertical Transition for Pyrrolocytosine in the Optimized Geometry of Its First Excited State,  $S_1$  (a  $\pi\pi^*$  State, Geometric Details Provided in Table 4), Pyrrolocytosine, in This  $S_1$  Geometry, Stacked with Guanine, as in B-Form DNA, and Pyrrolocytosine in Its  $S_1$  Geometry Hydrogen Bonded to Guanine<sup>a</sup>**

	CIS/6-31++G(d,p)		TDB3LYP/6-31++G(d,p)	
	$E/\text{eV}$	$f$	$E/\text{eV}$	$f$
PC alone in $S_1$ geometry	2.98	0.256	3.05	0.072
PC in $S_1$ geometry hydrogen bonded to G <sup>b</sup>	2.93	0.255	2.96	0.067
PC in $S_1$ geometry stacked with G	2.99	0.208	3.06	0.054

<sup>a</sup> The transition energies computed at the CIS level have been scaled by a factor of 0.72. <sup>b</sup> As the geometry of the  $S_1$  state is not identical to the geometry of the ground state, the geometry of the hydrogen-bonded complex formed is similar but not identical to that shown in Figure 2. The appropriate values for the bond lengths and angles, in the order given in Table 1, are 3.14, 2.96 and 2.97 Å and 179.3, 178.0 and 162.7°. The exact coordinates are given as Supporting Information.

**TABLE 7: Vertical Transitions Energies,  $E$ , and Oscillator Strengths,  $f$ , to Low-Lying States of Pyrrolocytosine and Guanine Stacked in Their Ground State Geometries as in B-Form DNA<sup>a</sup>**

CIS/6-31++G(d,p)			TDB3LYP/6-31++G(d,p)		
$E/\text{eV}$	$f$	assignment	$E/\text{eV}$	$f$	assignment
3.46	0.216	$\pi\pi^*$ on PC	3.53	0.053	$\pi\pi^*$ on PC
4.36	0.214	$\pi\pi^*$ on G	3.75	0.003	CT ( $\pi_G\pi_{PC}^*$ )

<sup>a</sup> The transition energies computed at the CIS level have been scaled by a factor of 0.72. States of charge-transfer character are reported as CT.

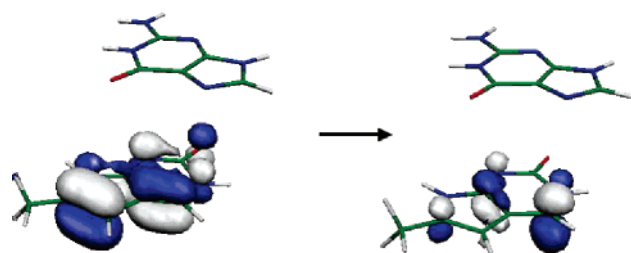


**Figure 5.** Guanine stacked above pyrrolocytosine as it would be in B-form DNA. At the CIS level, orbital involved in first  $\pi\pi^*$  transition are located on the pyrrolocytosine unit only.

transition is inversely related to the lifetime of the state with respect to that transition, the fluorescence lifetime of the  $\pi\pi^*$  state is predicted to be longer when it is involved in a base-stacked environment, and therefore the excited state is more likely to decay through some other, nonradiative process. Thus a base-stacking interaction appears to be a least partly responsible for the approximately 50% decrease in the fluorescence quantum yield of pyrrolocytosine observed when the base is in a double stranded segment of DNA, as opposed to a single stranded segment.<sup>3</sup>

## Conclusions

The hybridization and spectral and properties of a fluorescent base, pyrrolocytosine, have been computed for the first time. The base has been found to hydrogen bond to guanine in a manner analogous to that of cytosine. The interaction energy of the pyrrolocytosine:guanine complex was found to be  $-27.2 \text{ kcal mol}^{-1}$ . The vertical transitions energies, computed at the CIS/6-31++G(d,p) level, for transitions to the first two  $\pi\pi^*$  states in vacuo are 3.46 and 4.45 eV, in agreement with the experimentally determined peaks in the excitation spectrum of the base in aqueous solutions, 3.59 and 4.56 eV. The fully optimized geometry of the lowest energy  $\pi\pi^*$  state of pyrrolocytosine was located and found to be slightly more polar than the ground state and nonplanar. Fluorescence form this structurally relaxed  $\pi\pi^*$  state was predicted to occur at 2.98 eV, again in good agreement with the experimental data available.<sup>1,3</sup> The

appreciable fluorescence of pyrrolocytosine compared to that of cytosine is proposed to be caused by the significantly greater gap in energy between the lowest  $\pi\pi^*$  and  $n\pi^*$  states of pyrrolocytosine compared to cytosine. The results of our study suggest that the reduced fluorescence of pyrrolocytosine observed when the molecule is incorporated into a helical portion of nucleic acid results from an interaction with the bases stacked above (or below) pyrrolocytosine that reduces the oscillator strength for the transition from the  $\pi\pi^*$  excited-state back to the ground state. When pyrrolocytosine is hydrogen bonded to guanine no significant reduction in the oscillator strength for the transition was predicted.

**Acknowledgment.** The author thanks the Royal Society for funding, grant number 23699, the EPSRC, Computational Chemistry Working Party, for the award of computer time on the Columbus cluster and Prof. David Lilley and Dr. David Norman for helpful and stimulating discussions.

**Supporting Information Available:** Cartesian coordinates for the optimized ground-state geometry of: pyrrolocytosine obtained at the MP2/6-31G(d,p) and HF/6-31G(d,p) level, the first excited state,  $S_1$ , of pyrrolocytosine obtained at the CIS/6-31++G(d,p) level, the pyrrolocytosine:guanine hydrogen-bonded complex optimized at the HF/6-31G(d,p) level with  $C_s$  symmetry, the complex where the optimized  $S_1$  structure of pyrrolocytosine has been arranged with guanine as close as possible to the optimized structure for the ground-state hydrogen-bonded complex, and the structure of pyrrolocytosine stacked below guanine as it would be in B-form DNA. This information is available free of charge via the Internet at <http://pubs.acs.org>.

## References and Notes

- Berry, D. A.; Jung, K. Y.; Wise, D. S.; Serce, A. D.; Pearson, W. H.; Mackie, H.; Randolph, J. B.; Somers, R. L. *Tetrahedron Lett.* **2004**, 45, 2457.
- Daniels, M.; Hauswirth, W. *Science* **1971**, 171, 675.
- Lui, C.; Martin, C. T. *J. Mol. Biol.* **2001**, 308, 465.
- Lui, C.; Martin, C. T. *J. Biol. Chem.* **2002**, 277, 2725.
- David Lilley, University of Dundee, private communication.
- Becke, A. D. *J. Chem. Phys.* **1993**, 98, 5648.
- Lee, C. T.; Yang, W. T.; Parr, R. G. *Phys. Rev. B* **1988**, 37, 785.
- (a) Frisch, M. J.; Trucks, G. W.; Schlegel, H. B.; Scuseria, G. E.; Robb, M. A.; Cheeseman, J. R.; Zakrzewski, V. G.; Montgomery, J. A., Jr.; Stratmann, R. E.; Burant, J. C.; Dapprich, S.; Millam, J. M.; Daniels, A. D.; Kudin, K. N.; Strain, M. C.; Farkas, O.; Tomasi, J.; Barone, V.; Cossi, M.; Cammi, R.; Mennucci, B.; Pomelli, C.; Adamo, C.; Clifford, S.; Ochterski, J.; Petersson, G. A.; Ayala, P. Y.; Cui, Q.; Morokuma, K.; Malick, D. K.; Rabuck, A. D.; Raghavachari, K.; Foresman, J. B.; Cioslowski, J.; Ortiz, J. V.; Stefanov, B. B.; Liu, G.; Liashenko, A.; Piskorz, P.; Komaromi, I.; Gomperts, R.; Martin, R. L.; Fox, D. J.; Keith, T.; Al-Laham, M. A.; Peng, C. Y.; Nanayakkara, A.; Gonzalez, C.; Challacombe, M.; Gill, P. M. W.; Johnson, B. G.; Chen, W.; Wong, M. W.; Andres, J. L.; Head-Gordon, M.; Replogle, E. S.; Pople, J. A. *Gaussian 98*, revision A.7; Gaussian, Inc.: Pittsburgh, PA, 1998. (b) Frisch, M. J.; Trucks, G. W.; Schlegel, H. B.; Scuseria, G. E.; Robb, M. A.; Cheeseman, J. R.; Montgomery, J. A., Jr.; Vreven, T.; Kudin, K. N.; Burant, J. C.; Millam, J. M.; Iyengar, S. S.;

- Tomasi, J.; Barone, V.; Mennucci, B.; Cossi, M.; Scalmani, G.; Rega, N.; Petersson, G. A.; Nakatsuji, H.; Hada, M.; Ehara, M.; Toyota, K.; Fukuda, R.; Hasegawa, J.; Ishida, M.; Nakajima, T.; Honda, Y.; Kitao, O.; Nakai, H.; Klene, M.; Li, X.; Knox, J. E.; Hratchian, H. P.; Cross, J. B.; Adamo, C.; Jaramillo, J.; Gomperts, R.; Stratmann, R. E.; Yazyev, O.; Austin, A. J.; Cammi, R.; Pomelli, C.; Ochterski, J. W.; Ayala, P. Y.; Morokuma, K.; Voth, G. A.; Salvador, P.; Dannenberg, J. J.; Zakrzewski, V. G.; Dapprich, S.; Daniels, A. D.; Strain, M. C.; Farkas, O.; Malick, D. K.; Rabuck, A. D.; Raghavachari, K.; Foresman, J. B.; Ortiz, J. V.; Cui, Q.; Baboul, A. G.; Clifford, S.; Cioslowski, J.; Stefanov, B. B.; Liu, G.; Liashenko, A.; Piskorz, P.; Komaromi, I.; Martin, R. L.; Fox, D. J.; Keith, T.; Al-Laham, M. A.; Peng, C. Y.; Nanayakkara, A.; Challacombe, M.; Gill, P. M. W.; Johnson, B.; Chen, W.; Wong, M. W.; Gonzalez, C.; Pople, J. A. *Gaussian 03*, revision B.04; Gaussian, Inc.: Pittsburgh, PA, 2003.
- (9) Flükiger, P.; Lüthi, H. P.; Portmann, S.; Weber, J. *MOLEKEL 4.0*, Swiss Center for Scientific Computing: Manno, Switzerland, 2000.
- (10) Šponer, J.; Leszczynski, J.; Hobza P. *J. Phys. Chem.* **1996**, *100*, 1965.
- (11) For example Jensen, F. *Introduction to Computational Chemistry*; John Wiley & Sons: 1999.
- (12) Hobza, P.; Šponer, J. *Chem. Rev.* **1999**, *99*, 3247.
- (13) Kabeláč, M.; Hobza, P. *J. Phys. Chem. B* **2001**, *105*, 5805.
- (14) Broo, A.; Holmén, A. *J. Phys. Chem. A* **1997**, *101*, 3589.
- (15) Cramer, C. J. *Essentials of Computational Chemistry*; John Wiley & Sons: 2002.
- (16) Shukla, M. K.; Leszczynski, J. *J. Phys. Chem. A* **2002**, *106*, 11338.
- (17) Crespo-Hernández C. E.; Cohen, B.; Hare, P. M.; Kohler, B. *Chem. Rev.* **2004**, *104*, 1977.
- (18) Ismail, N.; Blancfort, L.; Olivucci, M.; Kohler, B.; Robb, M. A. *J. Am. Chem. Soc.* **2002**, *124*, 6818.
- (19) Merchán, M.; Serrano-Andrés L. *J. Am. Chem. Soc.* **2003**, *125*, 8108.
- (20) Tozer, D. J.; Amos, R. D.; Handy, N. C.; Roos, B. O.; Serrano-Andrés, L. *Mol. Phys.* **1999**, *97*, 859.
- (21) Parusel, A. B. J.; Rettig, W.; Sudholt, W. *J. Phys. Chem. A* **2002**, *106*, 804.
- (22) Sobolewski, A. L.; Domcke, W. *Chem. Phys.* **2003**, *294*, 73.
- (23) Dreuw, A.; Weisman, J. L.; Head-Gordon, M. *J. Chem. Phys.* **2003**, *119*, 2943.
- (24) Dreuw, A.; Head-Gordon, M. *J. Am. Chem. Soc.* **2004**, *126*, 4007.
- (25) Tawada, Y.; Tsuneda, T.; Yanagisawa, S.; Yanai, T.; Kimihiko, H. *J. Chem. Phys.* **2004**, *120*, 8425.
- (26) Jean, J. M.; Hall, K. B. *Proc. Natl. Acad. Sci. U. S.A.* **2001**, *98*, 37.
- (27) Jean, J. M.; Hall, K. B. *Biochemistry* **2002**, *41*, 13152.